Modeling of Soot Formation and Oxidation in Turbulent Diffusion Flames
P. J. Coelho and M. G. Carvalho

Modeling of Soot Formation and Oxidation in Turbulent Diffusion Flames

P. J. Coelho* and M. G. Carvalho†

Instituto Superior Técnico, 1096 Lisbon, Portugal

Soot concentration in a turbulent diffusion flame burning propane was predicted using several formation and oxidation models. The Favre-averaged equations governing conservation of mass, momentum, and energy and transport equations for turbulent quantities, mixture fraction and its variance were solved using the k-ε model and the laminar flamelet approach. Calculation of soot concentration was performed using the results of the flame field model as input data. The soot formation models of Khan and Greeves, and Moss and co-workers were used together with the soot oxidation models of Magnussen and Hjertager, Lee et al., and Nagle and Strickland-Constable. Comparison of the results with available measurements, and with the predictions obtained by Fairweather et al. using their own soot formation model, shows that reasonable predictions of soot concentration requires an adjustment of the constants of the model of Moss and co-workers. The soot formation model of Fairweather et al. appears to be less sensitive to the constants. The model of Khan and Greeves yields correct orders of magnitude, but fails to predict some important features of the data. Hence, there is a need to improve presently available soot formation and oxidation models to achieve a satisfactory predictive capability.

Nomenclature

A	=	constant in Magnussen and Hjertager model, Eq. (9)
C_d	=	constant in Lee et al. model, Eq. (10)
C_f, n	=	constants in Khan and Greeves model, Eq. (1)
$C_\alpha, C_\beta, C_\gamma, M_\alpha, M_\gamma, T_\alpha, T_\gamma$	=	constants in Steward et al. model, Eqs. (3–7)
C_2	=	constant in transport equation for ε
E	=	activation energy
f	=	mixture fraction
f_v	=	soot volume fraction
K_A, K_B, K_T, K_Z	=	rate constants in Nagle et al. model, Eqs. (11) and (12)
k, ε	=	turbulent kinetic energy and its dissipation rate
N_0	=	Avogadro number
n	=	soot particle number density
p_i	=	partial pressure of species i
R	=	gas constant, radial coordinate
S	=	source term of the transport equations
T	=	temperature
$\bar{w}$	=	mean oxidation rate
X	=	mole fraction
Z	=	axial coordinate
α, δ	=	nucleation rate
β	=	coagulation rate
γ	=	surface growth rate
ρ	=	density
ϕ	=	equivalence ratio

Subscripts

d	=	oxidation
f	=	formation
fu	=	fuel
in	=	inlet
O_2	=	oxygen
s	=	soot

Superscript

$-$	=	mean value

Introduction

THE problem of soot formation and oxidation has received significant attention due to its practical importance in combustion equipment and fire radiation. However, the complexity of the soot formation mechanisms has prevented the development of reliable modeling approaches. A detailed simulation of soot particle formation was developed by Frenklach and Wang,[1] including fuel pyrolysis, formation of polycyclic aromatic hydrocarbons (PAH), their planar growth and coagulation into spherical particles, surface growth, and oxidation of the particles. Miller et al.[2] described a model to calculate the concentration of PAH along streamlines of a laminar diffusion flame. The aromatic growth, inception, and oxidation phenomena were accounted for and their rates were derived from the fundamental chemical processes that occur in the flame combined with detailed measurements of species concentrations. Although these models have been successfully applied to several laminar and diffusion premixed flames, the complexity and the uncertainties about the physical processes involved preclude their application to engineering problems. The extension to turbulent flames would be even more complex due to the turbulence–chemistry interaction. Therefore, global soot models are presently employed in reactive flow problems of practical importance in engineering.

Global soot formation models are generally based either on one-step kinetic mechanisms or two-step mechanisms. A review of one-step kinetic mechanisms was presented by Mullins et al.[3] with emphasis placed on application to gas-turbine combustors. A simple kinetic expression often used in cal-

culations in furnaces and boilers is due to Khan and Greeves,[4] although it was originally developed for diesel engines. Tesner et al.[5] proposed a two-step mechanism where the first stage represents formation of radical nuclei, involving fuel cracking, branching, and coagulation steps, and the second stage describes formation of soot particles from the radical nuclei. This model was applied to turbulent acetylene–air flames[6] and to propane turbulent jet flames.[7]

The laminar flamelet approach has been the basis of recently developed soot formation models. A straightforward extension of the flamelet concept to soot volume fraction is not possible. Gore and Faeth[8] have shown that calculations based on a relationship between soot volume fraction and mixture fraction yields reasonable predictions in the overfire region. A similar approach was followed by Kent and Honnery,[9] who established the relationship between instantaneous soot volume fraction and mixture fraction from measurements in turbulent flames. They concluded that in the lower parts of the flame this formulation is not adequate and a finite reaction rate model is needed. The maximum soot concentrations further up the flame are less dependent on residence time and a mixture fraction approach may be useful there.

Kennedy and co-workers[10–12] developed a simple model for the prediction of soot concentration in laminar diffusion flames based on the solution of a single transport equation for soot volume fraction, accounting for the processes of nucleation, surface growth, and oxidation. Rates of these processes are functions of mixture fraction. The rate of nucleation is modeled as a Gaussian distribution in mixture fraction and the surface growth rate is determined using an empirical correlation between mixture fraction and the specific surface growth rate. This correlation is obtained from measurements.[13] The particle number density, required for calculation of the surface growth rate, is taken as an average value from measurements.[13]

Honnery and Kent[14] also solve a transport equation for soot mass fraction along particle trajectories, in which the soot growth rate is determined from a correlation of specific surface growth rate against temperature and mixture fraction, based on experimental data.[15] The particle number density is not prescribed, as in the model of Kennedy and co-workers, but there is no need to solve a transport equation for this quantity because the variation in particle number density is accounted for by the use of a relationship between surface area and soot volume fraction developed by Honnery et al.[15]

Moss et al.[16,17] presented a model based on the solution of transport equations for the soot particle number density and soot mass fraction. The rates of nucleation, coagulation, and surface growth are expressed as functions of mixture fraction. The constants of the model were determined from numerical experiments to optimize the predictions of a laminar diffusion flame of ethylene. A modification of the surface growth term was later proposed to cope with experimental evidence in methane[18] and prevaporized kerosene flames.[19]

Jones, Lindstedt, and co-workers[20–22] proposed a model based on the solution of the same transport equations and on the simulation of the same physical phenomena of Moss and co-workers model. However, they assume that nucleation and surface growth rates are related to the concentration of a characteristic pyrolysis product, taken as acetylene, rather than the concentration of fuel. The model was successfully applied to counterflow diffusion flames of ethylene and propane,[20] a turbulent natural gas jet in a crosswind[21] and to a turbulent diffusion propane flame.[22]

The assumption that soot formation is directly related to a characteristic pyrolysis product—acetylene—rather than the parent fuel, which is supported by experimental evidence, has also been employed recently by Missaghi et al.[23] They use a reduced kinetic mechanism to predict the formation of acetylene and simulate the formation of benzene, PAH growth, and its conversion to soot as in Frenklach and Wang's model.

Most of the soot formation models referred to previously rely on empirical correlations or involve coefficients that were determined from data acquired in individual flames. Therefore, application of these models to different flames is questionable. However, the prediction of reactive flows in combustion systems, where radiation from soot is often dominant, requires the incorporation of a soot formation model whose dependency on the fuel and flame conditions is either negligible or well known. Moreover, the model should be simple enough to allow its incorporation in a computational fluid dynamics (CFD) code for a reactive flow without significant increase in computational and memory requirements.

The objective of this work is to compare several soot formation models and investigate their suitability for incorporation in a reactive flow code for simulation of combustion equipment. Given the constraints outlined above, three models were selected for comparison: the models of Khan and Greeves,[4] Stewart et al.[19] and Fairweather et al.[22] We have performed calculations using only the first two models. However, predictions obtained by Fairweather et al. for the flame considered in the present study are shown for comparison purposes. The models are evaluated by means of comparison between predictions and measurements published in the literature[24] for soot concentration in a propane turbulent diffusion flame.

Most of the works mentioned previously include a model of soot oxidation. Oxidation by molecular oxygen has been modeled using the semiempirical formula of Nagle and Strickland-Constable[25] (see, e.g., Refs. 1, 2, 12, 14, and 18), the expression due to chemical kinetics proposed by Lee et al.[26] (see, e.g., Refs. 20–22), and the model of Magnussen and Hjertager,[6] which is based on the assumption that the oxidation rate is controlled by the mixing rate of air and fuel. These three models were employed in the present study. More recently, several authors have pointed out that molecular oxygen is not the only species responsible for soot oxidation. The role of OH radicals may be significant[27,28] and was accounted for in some of the works mentioned earlier.[1,2,12,14] Other species, such as O, H, NO, H_2O, and CO_2 may also play a role.[14,23,29]

The soot formation and oxidation models employed in this work are presented in the next section after a brief description of the model used to calculate the velocity and temperature fields and the chemical species concentrations. The results obtained are then presented and discussed and this article ends with a summary of the main conclusions.

Mathematical Models

Governing Equations, Turbulence, and Combustion Models

The model employed to calculate the velocity and temperature fields and the species concentrations distributions is based on the numerical solution of the density-weighted average form of the equations governing conservation of mass and momentum and transport equations of scalar quantities.

The k-ε eddy viscosity/diffusivity model was employed to close these equations. Standard values were used for all the constants except for constant C_2 in the transport equation for the dissipation rate of turbulent kinetic energy. The configuration of the flame studied in this work is similar to a round jet whose spreading rate is overestimated by first- and second-moment closures. Several modifications of the k-ε model have been proposed to overcome this problem in isothermal round jets.[30] Here, we have simply reduced C_2 to 1.75. Fairweather et al.,[22] who employed a second-moment closure to model the flame experimentally studied by Nishida and Mukohara,[24] also reduced C_2 to bring the predicted flame spreading rate into agreement with measurements.

Combustion was modeled using the conserved scalar/prescribed probability density function (PDF) formalism. The mixture fraction was the scalar chosen and a clipped Gaussian

shape was assumed for the PDF of mixture fraction. The laminar flamelet model was used to relate temperature and species concentrations to mixture fraction. Different flamelet libraries were used according to the air preheat temperature. The resultant relations between temperature and mixture fraction are valid for an adiabatic flame, but do not hold for a sooting flame due to the radiative heat loss. Therefore, a method has to be devised to relate temperature to mixture fraction accounting for heat losses.

It is possible to use a model to calculate soot concentration and to estimate the radiative heat transfer. Then, an energy equation may be solved and a relationship between instantaneous values of enthalpy and mixture fraction assumed to compute flame temperature taking into account the radiative heat loss. This coupling has been employed to model laminar diffusion flames of ethylene[31] and acetylene.[32] It was found that in strongly radiating flames there is a strong interaction between radiation and soot kinetics and the relationships between temperature and mixture fraction vary significantly at different locations and affect the soot kinetics processes.[32] Therefore, it is crucial to calculate the local fraction of radiative heat loss.

However, in case of turbulent flames the role played by turbulent fluctuations complicates the problem. In fact, soot formation and oxidation are strongly dependent on temperature. Therefore, temperature and soot distributions both depend one on the other. Soot concentration influences radiation, which influences enthalpy and, therefore, temperature and soot concentration.[32] Supposing that soot formation and oxidation models are accurate enough to predict a correct distribution of soot concentration, it may happen that modeling assumptions concerning the influence of turbulence/radiation interaction or enthalpy/mixture fraction relationship yield an inaccurate temperature field. In such a case, predicted soot concentration would be poorly predicted because the temperature field was not correct.

Gore et al.[33] developed a coupled flame structure and radiation analysis of turbulent diffusion, strongly radiating acetylene/air flames. They used a multiray method accounting for turbulence/radiation interaction and they assumed a joint PDF of the mixture fraction and enthalpy. They used an extension of the laminar flamelet concept to estimate soot volume fraction. According to the findings of Sivathanu and Gore,[32] this coupling procedure is very important in strongly radiating flames, since the fraction of radiative heat loss may exceed 50%.

However, in propane flames the fraction of radiative heat loss is much smaller. Moreover, the coupling procedure applied to turbulent flames requires modelling assumptions concerning the interaction between turbulence and radiation and the enthalpy/mixture fraction relationship. Here, attention is focused on the evaluation of soot formation models and, therefore, we decoupled soot from flame structure predictions. A simple method[34] was used to adjust flamelet temperatures as a function of mixture fraction such that peak mean temperatures are in agreement with the measurements. The same procedure was used in some of the works mentioned in the Introduction.[18,20-22]

The governing equations are discretized using a finite volume/finite difference method and solved using the SIMPLE algorithm. The results obtained are used as input data for the subsequent solution of transport equations for the soot particle number density, when the soot formation model involves this quantity, and soot mass fraction. The soot formation and oxidation models employed in this work are briefly described next.

Soot Formation Models

Khan and Greeves[4]

This model uses a simple kinetic rate expression to model soot formation. The source term of the transport equation for soot mass fraction is given by

$$S_f(m_s) = C_f p_{fu} \phi^n \exp(-E/RT) \tag{1}$$

ϕ, p_{fu}, and T may be related to mixture fraction and the mean value of the source term is computed by integration:

$$\bar{S}_f = \bar{\rho} \int_0^1 \frac{S_f}{\rho} p(f) \, df \tag{2}$$

Soot formation occurs only for values of ϕ in the range $\phi_{min} \leq \phi \leq \phi_{max}$, where ϕ_{min} stands for the incipient sooting limit and ϕ_{max} is a value above which soot formation becomes negligible.

Stewart et al.[19]

This model solves transport equations for n and soot mass fraction m_s, whose source terms are calculated as follows:

$$S_f\left(\frac{n}{\rho N_0}\right) = \alpha - \beta \left(\frac{n}{N_0}\right)^2 \tag{3}$$

$$S_f(m_s) = \gamma f_v^{2/3} n^{1/3} + \delta \tag{4}$$

$$\alpha = C_\alpha \rho^2 T^{1/2} X_{fu}^{M\alpha} \exp\left(\frac{-T_\alpha}{T}\right) \tag{5}$$

$$\beta = C_\beta T^{1/2} \tag{6}$$

$$\gamma = C_\gamma \rho T^{1/2} X_{fu}^{M\gamma} \exp\left(\frac{-T_\gamma}{T}\right) \tag{7}$$

$$\delta = 144\alpha \tag{8}$$

where C_α, C_β, C_γ, M_α, M_γ, T_α, and T_γ are constants of the model. The two terms on the right-hand side (RHS) of Eq. (3) describe the processes of nucleation and coagulation, respectively, and the two terms on the RHS of Eq. (4) represent the contributions of surface growth and nucleation. Equation (2) is employed to calculate the mean values of the source terms.

Fairweather et al.[22]

This model simulates the same physical phenomena and solves the same transport equations of the previous model, but the formation rates are related to the concentration of a product of pyrolysis, taken to be acetylene, rather than to the parent fuel. We did not perform computations using this model, but since it was applied in Ref. 22 to the same flame that we are studying here, we include a comparison of those predictions together with the ones that we have obtained using the first two models against experimental data.[24]

Soot Oxidation Models

Magnussen and Hjertager[6]

This model assumes that turbulence decay controls the rate of soot oxidation. The source term is computed as the minimum of two expressions, one appropriate in regions where the local mean soot concentration is low compared to the oxygen concentration and the other applicable to regions where oxygen concentration is low and limits the oxidation rate:

$$S_d = \min\left(A m_s \rho \frac{\varepsilon}{k}, \; A \frac{m_{O_2}}{s_s} \frac{m_s s_s}{m_s s_s + m_{fu} s} \rho \frac{\varepsilon}{k}\right) \tag{9}$$

Lee et al.[26]

This model estimates the rate of soot oxidation using a simple kinetic rate expression

$$S_d = C_d m_s (p_{O_2}/\sqrt{T}) \exp(-E/RT) \qquad (10)$$

Nagle and Strickland-Constable[25]

The rate of oxidation of soot particles (g cm^{-2} s^{-1}) is given by

$$\bar{w} = 12 \left[\left(\frac{K_A p_{O_2}}{1 + K_Z p_{O_2}} \right) x + K_B p_{O_2}(1 - x) \right] \qquad (11)$$

where

$$x = [1 + (K_T/p_{O_2} K_B)]^{-1} \qquad (12)$$

The source terms of the transport equations for soot particle number density and soot mass fraction may be obtained from Eq. (11).[18]

Results and Discussion

The models outlined previously were applied to a confined propane/air turbulent diffusion flame experimentally studied by Nishida and Mukohara.[24] Propane at ambient temperature is introduced into a combustion chamber with an internal diameter of 115 mm through a nozzle of i.d. 2.0 mm at an average velocity of 30 m/s. Air is supplied through an annulus surrounding the nozzle. Results are presented for two cases:

in the first case, T_{in} and the average velocity are 50°C and 0.40 m/s, respectively; in the second case, the inlet air temperature and the average velocity are 500°C and 0.96 m/s, respectively.

Calculations were performed using two different grids with 61 × 34 and 122 × 68 grid nodes. It was found that the predicted results are only marginally influenced by grid refinement. Typical results of this influence will be shown next.

Temperature and Oxygen Concentration

The source terms of the transport equation for soot mass fraction, describing the soot formation and oxidation processes, are strongly dependent on the temperature and oxygen concentration. Therefore, an accurate prediction of these quantities is required to evaluate the soot formation and oxidation models.

Figure 1 shows predicted radial temperature profiles along with the measurements for the two cases studied. To illustrate the influence of grid refinement on the predictions, both solutions obtained for T_{in} = 500°C were plotted. It can be seen that they are very close to each other and, therefore, the results can be considered as grid independent for evaluation purposes.

The flame width is slightly overpredicted. In fact, the computed peak temperature at z = 100 mm occurs at a larger distance from the centerline. The centerline temperature is underestimated up to z = 300 mm for T_{in} = 500°C, but a good agreement was found for T_{in} = 50°C.

The effect of the reduction of constant C_2 of the turbulence model is an increase of the dissipation rate of the turbulent kinetic energy and a decrease of the turbulent viscosity, yielding larger temperature gradients and a lower spreading rate of the jet. Therefore, the decrease of constant C_2 improves the temperature prediction at the outer flame edge, but at the expense of a decrease of the centerline temperature. The selected value for C_2 is the best compromise between the predictions of centerline temperature and flame width.

A detailed analysis of turbulence, combustion, and radiative heat transfer models as well as their interaction is needed to further improve the predictions, but this is out of the scope of the present study. The level of agreement between measured and predicted temperatures is comparable to that obtained by Fairweather et al.,[22] who employed the same combustion model, but a second-order moment closure for the turbulent fluxes. As in their calculations, we have also over-
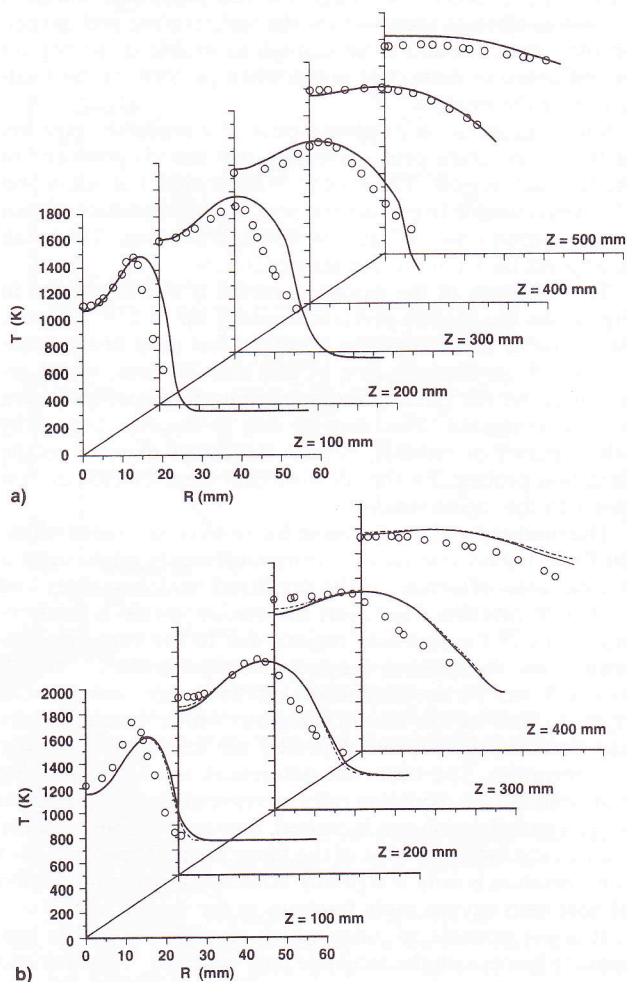

Fig. 1 Predicted and measured radial temperature profiles (solid lines: predictions, coarse grid; dashed lines: predictions, fine grid; and symbols: measurements[24]). T_{in} = a) 50 and b) 500°C.
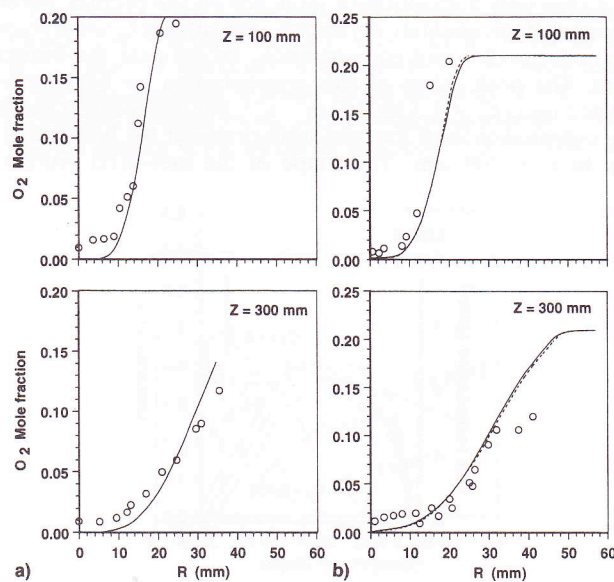

Fig. 2 Radial profiles of predicted and measured oxygen mole fraction (solid lines: predictions, coarse grid; dashed lines: predictions, fine grid; and symbols: measurements[24]). T_{in} = a) 50 and b) 500°C.

predicted the centerline temperature at axial stations beyond 0.5 m (not shown here). This has been attributed to the radiative heat loss treatment.

The computed oxygen mole fraction profiles at $z = 100$ and 300 mm are displayed in Fig. 2 together with the experimental data. The oxygen mole fraction is reasonably well predicted but, contrary to the calculations, small amounts of oxygen were measured within the flame region. A similar behavior was found in the calculations of Fairweather et al.[22] The influence of grid refinement on the predictions is negligible.

On the whole, the predictions of temperature and oxygen mole fraction up to $z = 500$ mm are satisfactory and sufficiently close to the data to allow the comparison of soot formation and oxidation models presented next. An exception is the oxygen mole fraction in the reacting region, which is close to zero according to the predictions, and small, but not zero, according to the measurements.

Soot Formation Model of Khan and Greeves

Khan and Greeves[4] soot formation model was applied to the flame under consideration using three different values of constant C_f of the model:

1) $C_f = 0.468$ kg N^{-1} m^{-1} s^{-1}, the value originally employed by Khan and Greeves in the calculation of soot formation in a diesel engine, neglecting soot combustion.

2) $C_f = 0.84$ kg N^{-1} m^{-1} s^{-1}, a value tuned by Abbas[35] to fit experimental data.[36]

3) $C_f = 1.5$ kg N^{-1} m^{-1} s^{-1}, a value also tried by Abbas that is close to $C_f = 1.376$ kg N^{-1} m^{-1} s^{-1}, a value employed by Khan and Greeves when soot oxidation was accounted for. In a later work[37] Abbas suggested that C_f is proportional to the Richardson number and took the numerically optimized proportionality constant equal to 2.54×10^6 kg N^{-1} m^{-1} s^{-1}. This yields C_f values higher than the previously mentioned ones, overpredicting significantly soot concentration for the propane flame considered here. This may be due to the fact that this proportionality constant was selected to fit measurements in acetylene flames[35] whose soot propensity is greater than in propane flames.

Figure 3 shows the calculated centerline evolution of soot concentration for $T_{in} = 50°C$. Soot concentration increases rapidly in the initial flow region, reaches a maximum between $z = 200–300$ mm, and decreases farther downstream due to soot oxidation. All these features are correctly predicted by the model. A similar behavior was found for $T_{in} = 500°C$.

C_f has only a quantitative influence on the profiles whose shape remains qualitatively similar. The smaller C_f value tends to underpredict soot concentration, except near the burner exit. The peak values of soot concentration are better estimated using $C_f = 1.5$ kg N^{-1} m^{-1} s^{-1}, but this constant yields an overprediction of soot concentration near the burner exit, up to $z = 200$ mm. The shape of the measured profiles,

namely the increase of soot concentration from the burner exit up to the peak, is not adequately described by the model, despite of the value selected for C_f. This is not surprising regarding the simplicity of the model and the complexity of the phenomena that it attempts to describe. But it is important to point out that the model at least allows a correct estimation of the order of magnitude of soot concentration. The value $C_f = 1.5$ kg N^{-1} m^{-1} s^{-1} was employed in all the following calculations.

Beyond $z = 500$ mm soot concentration is underpredicted for $T_{in} = 50°C$. This can be explained by the temperature overestimation beyond $z = 500$ mm (not shown in Fig. 1) and corresponding increase of the oxidation rate. The overprediction of temperature in that region, caused by the assumption of a constant fraction of radiative heat loss, does not influence the soot concentration predictions shown here up to $z = 500$ mm.

No attempt was made to change the constant $n = 3$ and the activation temperature $E/R = 20,000$ K, which have been employed in all previous studies. However, the instantaneous soot formation rate plotted as a function of mixture fraction (not shown here) exhibits a peak for a mixture fraction of 0.32. This value is larger than those found by others[12,15] and suggests that the exponent $n = 3$ is too high. This may be responsible for the prediction of a faster increase of soot concentration near the burner exit when compared with the measurements.

Predicted and measured profiles of soot concentration are shown in Fig. 4. The three different oxidation models mentioned earlier were used. The influence of the grid on the computed results is shown, as an example, for the axial profiles at $T_{in} = 500°C$. Although the two numerical solutions are not as close as observed for the temperature and oxygen profiles, they are still close enough to enable us to neglect the influence of numerical errors when performing the evaluation of the models.

Soot concentration exhibits a peak just inside the position of the temperature peak, revealing that soot is produced in the fuel-rich region. The soot formation model of Khan and Greeves is unable to predict the peak in radial profiles of soot concentration observed at $z = 100$ and 200 mm. This peak disappears far from the burner exit.

The influence of the oxidation model is also illustrated in Fig. 4. All the models perform similarly up to $z = 200$ mm. At the outer flame edge the observed fast drop of soot concentration, particularly at $z = 200$ and 300 mm, is not reproduced by the predictions, suggesting that soot oxidation is underestimated. This may be due to the role played by other species or radicals, besides molecular oxygen, on the oxidation process. Farther downstream the predicted drop is closer to the measurements.

The prediction of oxygen mole fractions close to zero within the flame region, contrary to the measurements, might suggest a noticeable influence on the predicted oxidation rates and soot concentration. However, the oxidation rate is predominant only in the fuel-lean regions due to the very low concentrations of oxygen in the fuel-rich regions of the flame.[32] To check this, we have artificially set the oxygen mole fraction equal to 0.02 in the fuel-rich regions where smaller values had been calculated, and repeated the calculations of soot concentration. The observed differences are small, proving that although the oxidation rates increase in the regions where oxygen mole fraction was increased, they are still much smaller than on the fuel-lean edge of the flame front. Therefore, soot concentration is only marginally influenced by the prediction of near-zero oxygen mole fractions in the fuel-rich regions.

It is not possible to judge which oxidation model is performing better with the available data since the formation and oxidation processes are interrelated. Therefore, e.g., an overprediction of soot concentration may be due either to an overprediction of soot formation or an underprediction of soot
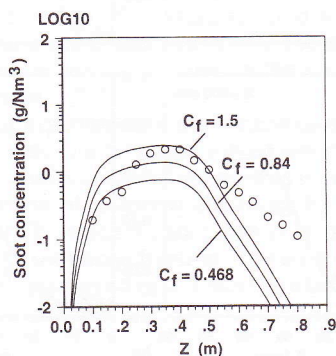
Fig. 3 Influence of constant C_f (kg N^{-1} m^{-1} s^{-1}) of Khan and Greeves[4] soot formation model on the predicted soot concentration for $T_{in} = 50°C$.
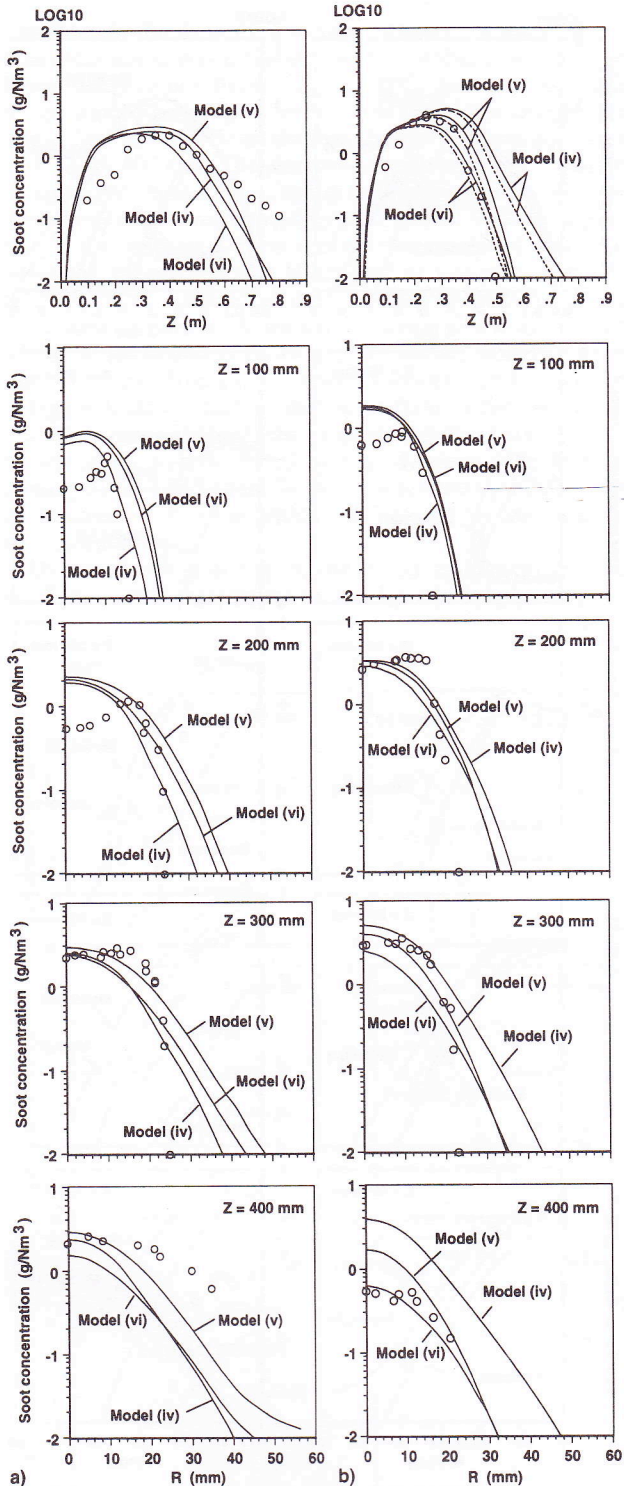
Fig. 4 Predicted (solid lines: coarse grid and dashed lines: fine grid) and measured (symbols) soot concentration profiles using the soot formation model of Khan and Greeves,[4] and three different oxidation models (Magnussen et al.,[6] Lee et al.,[26] and Nagle et al.[25]). T_{in} = a) 50 and b) 500°C.

oxidation. However, the predictions show that for the present flame the different oxidation models broadly yield qualitatively similar results.

On the whole, regarding the simplicity of this soot formation model and the complexity of the soot formation processes, the agreement between the predictions and the measurements may be considered good. However, there are several features of the data that are not reproduced by the predictions, as explained earlier.

Soot Formation Model of Stewart et al.[19]

The soot formation model of Moss and co-workers[18,19] was evaluated next. The sets of constants optimized for the predictions of a laminar diffusion prevaporized kerosene flame[19] and a buoyant turbulent diffusion flame of methane[18] were tried. In both cases the model fails to predict the peak soot concentration levels by at least two orders of magnitude. Soot concentration is overpredicted in the first case and underpredicted in the second one. Moreover, the slightly different model used earlier by Moss et al.[16,17] was also implemented together with the constants employed therein. Although better predictions are obtained, there is still a discrepancy of about one order of magnitude in the soot peak concentration. This shows that the applicability of the model is questionable under conditions different from those under which the constants were calibrated. This is an undesirable feature of the model.

To apply the model to the flame studied here, several numerical experiments were carried out with different constants and the following was the selected set:

$$C_\alpha = 10^4 \text{ m}^3 \text{ K}^{-1/2} \text{ kg}^{-2} \text{ s}^{-1}, \quad C_\beta = 6 \times 10^{13} \text{ m}^3 \text{ K}^{-1/2} \text{ s}^{-1}$$

$$C_\gamma = 1 \text{ m K}^{-1/2} \text{ s}^{-1}$$

$$T_\alpha = 21,000 \text{ K}, \quad T_\gamma = 12,600 \text{ K}, \quad M_\alpha = M_\gamma = 1$$

The values used for the activation temperature for nucleation T_α and surface growth rate T_γ are equal to those employed by Stewart et al.[19] Fairweather et al.[22] also used similar activation temperatures. The nucleation and surface growth rates were assumed to be linearly related to the fuel mole fraction, i.e., $M_a = M_\gamma = 1$, as in Syed et al.[18] Stewart et al.[19] increased the exponents M_α and M_γ to shift the maximum rates to richer mixtures, as if the rates were dependent on an intermediate species rather than the parent fuel. However, in the present case, when M_α and M_γ are increased, the rate of increase of soot concentration along the centerline in the neighborhood of the burner is overestimated. This does not occur when $M_\alpha = M_\gamma = 1$. Moreover, Fairweather et al.,[21] who have assumed that the nucleation and surface growth rates are linearly related to an intermediate species, acetylene, have found that the peaks of these rates occur at a mixture fraction of about 0.10. Their predicted variation of the instantaneous rate terms as a function of mixture fraction is qualitatively similar to our prediction, displayed in Fig. 5.

Constants C_α and C_β were adjusted coherently to yield peak values of soot particle number density of the order of 10^{17} m^{-3}. Values of this order of magnitude are generally found in the measurements available in the literature.[19,38] This observation is the basis for the prescription of an average particle number density in the model of Kennedy et al.[10-12] The pre-
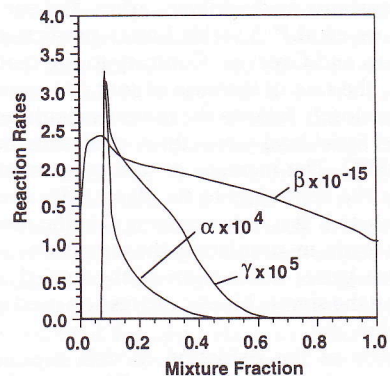

Fig. 5 Instantaneous nucleation ($\alpha \times 10^4$ m^{-3} s^{-1}), coagulation ($\beta \times 10^{-15}$ m^3 s^{-1}) and surface growth ($\gamma \times 10^5$ kg m^{-2} s^{-1}) rate terms as a function of mixture fraction for T_{in} = 50°C.
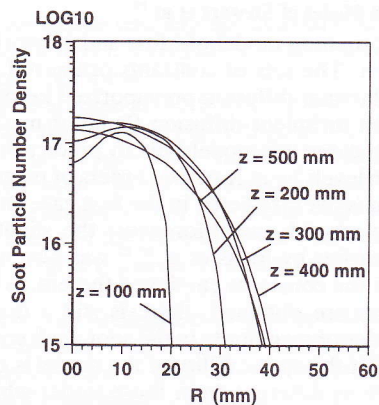
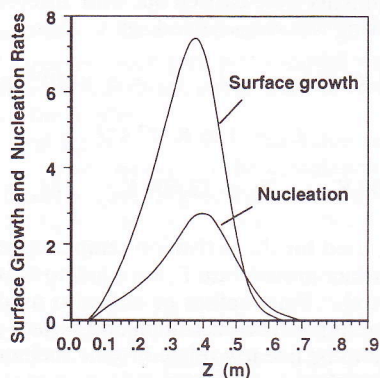Fig. 6 Predicted radial profiles of soot particle number density for $T_{in} = 50°C$.

Fig. 7 Predicted evolution of the surface growth and nucleation rates (kg m^{-3} s^{-1}) along the centerline for $T_{in} = 50°C$.

dicted radial profiles of soot particle number density are shown in Fig. 6.

Constant C_γ was tuned together with C_α and C_β to give soot concentration profiles close to the measurements and to provide a dominance of surface growth rate relative to nucleation rate, as observed in most laminar diffusion flames.[39] The predicted rates of surface growth and nucleation are displayed in Fig. 7. The peak of surface growth is about three times larger than the peak of nucleation rate. Both rates increase up to $z = 400$ mm, with the surface growth prevailing over the nucleation rate, and decrease farther downstream. These evolutions are consistent with those calculated by Stewart et al.[19]

The calculations performed using the set of constants listed previously are illustrated in Fig. 8, which shows predicted soot concentration profiles along with the measurements using the three different oxidation models. It can be seen that, after tuning the constants as described earlier, the soot formation model of Moss et al.[18,19] yields better predictions than the model of Khan and Greeves. Contrary to the model of Khan and Greeves, the rate of increase of soot concentration along the centerline closely follows the measurements, except when the Nagle and Strickland-Constable[25] oxidation model is used and $T_{in} = 500°C$. The increase of soot concentration at $z = 100$ mm from the centerline to the flame edge is also reasonably well predicted. It is not surprising that the model of Moss et al.[18,19] succeeds in simulating these features since it embodies a much better description of the underlying physical processes than the simple kinetic expression used in Khan and Greeves model.

The behavior of the oxidation models is similar to that observed previously together with the Khan and Greeves[4] soot formation model. But now, for $T_{in} = 500°C$, the Nagle and Strickland-Constable oxidation model significantly underestimates soot concentration, suggesting a too high oxidation
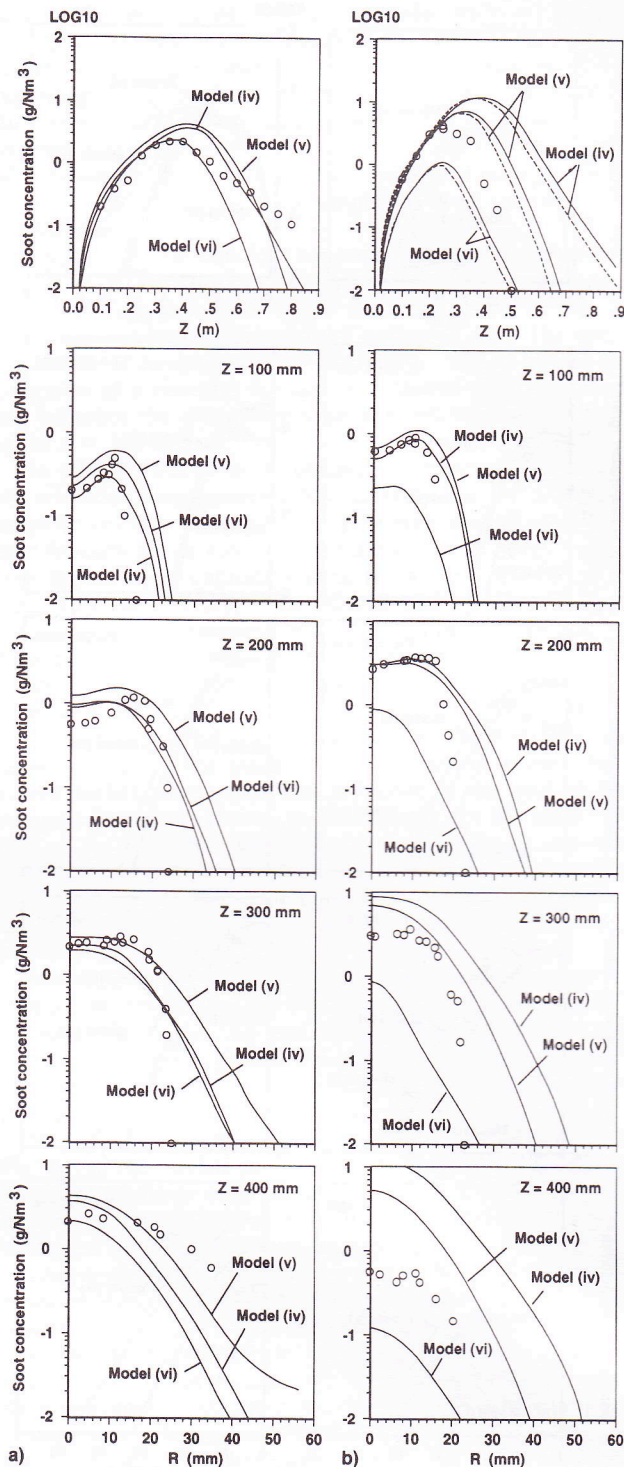

Fig. 8 Predicted (solid lines) and measured (symbols) soot concentration profiles using the soot formation model of Stewart et al.[19] and three different oxidation models (Magnussen et al.,[6] Lee et al.,[26] and Nagle et al.[25]). $T_{in} =$ a) 50 and b) 500°C.

rate, as also observed by others.[2] In fact, the role played by soot oxidation can be observed even at $z = 100$ mm. At this axial station the soot concentration computed using Nagle's model is already smaller than using the other models, especially for $T_{in} = 500°C$. This can only be attributed to the soot oxidation model. This is an interesting result because the predicted mean oxygen concentration is near-zero in this region. But, due to turbulent fluctuations, the oxidation rate is not zero.

However, there is an important feature of the measured soot concentration profiles that only Nagle's model is able to

simulate. At the downstream cross section ($z = 400$ mm) soot concentration is much higher and the profile is wider in the lower temperature flame ($T_{in} = 50°C$) than in the higher temperature flame ($T_{in} = 500°C$). For the higher temperature flame there is a significant decrease in soot concentration from $z = 300$ to 400 mm. This decrease is only correctly simulated using Nagle's model, although at both axial stations soot concentration is underestimated by that model. Soot concentration at $z = 300$ and 400 mm is of the same order of magnitude when the Magnussen and Hjertager[6] or Lee et al.[26] models are employed. Therefore, these models seem to underestimate soot oxidation. A similar behavior was also observed when the Khan and Greeves soot formation model was used instead of the Moss and co-workers model (see Fig. 4).

Figure 8 shows that at the outer flame edge, where the oxidation rate is higher, the measured drop of soot concentration is not well predicted by any of the models. This had already been observed in Fig. 4 and is related to shortcomings of the oxidation models, which only account for oxidation due to molecular oxygen.

Overall, looking at Fig. 8, the better agreement between predictions and measurements can be attributed to the oxi-

dation models of Magnussen and Hjertager and Lee et al. But the discussion has shown that none of the oxidation models used here is performing satisfactorily.

Comparison of Soot Formation Models

Finally, in Fig. 9, the predictions published by Fairweather et al.[22] were plotted together with our predictions obtained using the soot formation models[4,19] discussed earlier. As a basis for comparison the soot oxidation model of Lee et al.[26] was chosen since it was used in the work of Fairweather et al.

The figure shows that, after tuning the constants appropriately, the soot formation model of Moss and co-workers[18,19] yields better predictions than Khan's model. In fact, the rate of increase of soot concentration along the centerline in the initial flow region and the radial profile of soot concentration near the centerline, at $z = 100$ and 200 mm, are much better predicted using the model of Moss et al.,[18,19] which simulates correctly the radial peak of soot concentration. Khan's model is unable to predict this behavior. Although this region is only a portion of the flame, it is the region where the comparison between the soot formation models is easier to perform because soot formation dominates over soot oxidation. The superiority of the model of Moss et al.[18,19] is not surprising since it simulates the processes of nucleation, surface growth, and coagulation, whereas the model of Khan et al. relies on a simple kinetic expression.

As far as the model of Fairweather et al. is concerned, Fig. 9 shows that it significantly underestimates soot concentration in the flow region near the burner, but it performs similarly to the other soot formation models farther downstream. This model had been applied previously to laminar counterflow ethylene and propane flames,[20] laminar acetylene/air and acetylene-methane/air diffusion flames,[32] and it was applied almost in the same form to the propane flame considered here.[22] Only the oxidation rate constant was modified. Therefore, the agreement between the predictions obtained using this soot formation model and the measurements suggests that Fairweather's model is much less sensitive to different flames and conditions than the model of Moss and co-workers.[18,19] This may be due to the fact that Fairweather et al. assume a direct relation between the nucleation, surface growth, and coagulation rates and a product of fuel pyrolysis—acetylene—as experimentally observed. The small sensitivity of the constants of the model to different flame conditions is a desirable feature and an advantage of Fairweather's model over the model of Moss and co-workers.

Conclusions

Several soot formation and oxidation models were applied to the prediction of soot concentration in a propane turbulent diffusion flame. From the analysis carried out the following conclusions may be drawn:

1) Khan and Greeves soot formation model, despite its simplicity and limited physical basis, yields correct orders of magnitude of soot concentration, but it is not adequate if reasonably good quantitative predictions are sought.

2) The soot formation model of Moss and co-workers yields better predictions of soot concentration than the Khan and Greeves model when the constants are tuned appropriately. However, the application to a flame different from the one used to calibrate the constants may result in significant errors.

3) The soot formation model of Fairweather et al. appears to be much less sensitive to the set of constants than the Moss and co-workers model, and, given its better physical basis, it has a good potential for application to different flames.

4) None of the soot oxidation models employed here simulates adequately the measured trends. The Nagle and Strickland-Constable model tends to overestimate soot oxidation and the Magnussen and Hjertager and Lee et al. models underestimate that rate. The drop of soot concentration at the
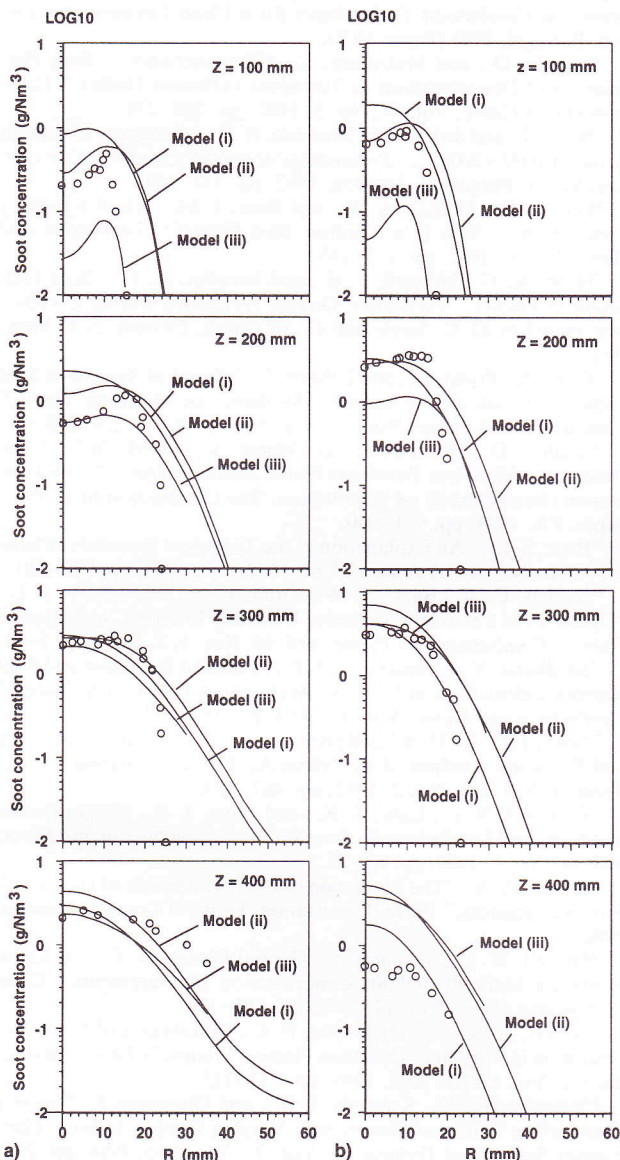

Fig. 9 Predicted (solid lines) and measured (symbols) soot concentration profiles using the soot formation models of Khan and Greeves,[4] Stewart et al.,[19] and Fairweather et al.,[22] and the soot oxidation model of Lee et al.[26] T_{in} = a) 50 and b) 500°C.

outer flame edge was not correctly predicted by the models, suggesting that other oxidizing species, such as OH, need to be taken into account.

5) As far as the application to a CFD code for reactive flows is concerned, the application of the soot formation model of Moss and co-workers can only be recommended if the constants were tuned for a similar flame. If the combustion model is able to compute acetylene, the model of Fairweather et al. is an alternative. In any case, the model of Khan and Greeves is expected to estimate the correct orders of magnitude of soot concentration, but unable to accurately simulate its distribution.

6) Despite the progress achieved during the last few years, there is still a lot of work to do before soot formation and oxidation models have achieved a level of accuracy and reliability comparable with presently available turbulence and combustion models.

References

[1]Frenklach, M., and Wang, H., "Detailed Modeling of Soot Particle Nucleation and Growth," *23rd Symposium (International) on Combustion*, The Combustion Inst., Pittsburgh, PA, 1990, pp. 1559–1566.

[2]Miller, J. H., Honnery, D. R., and Kent, J. H., "Modeling the Growth of Polynuclear Aromatic Hydrocarbons in Diffusion Flames," *24th Symposium (International) on Combustion*, The Combustion Inst., Pittsburgh, PA, 1992, pp. 1031–1039.

[3]Mullins, J., Simmons, B., and Williams, A., "Rates of Formation of Soot from Hydrocarbon Flames and Its Destruction," CP-422, AGARD, 1987 (Paper 23).

[4]Khan, I. M., and Greeves, G., "A Method for Calculating the Formation and Combustion of Soot in Diesel Engines," *Heat Transfer in Flames*, edited by N. H. Afgan and J. M. Beer, Scripta, Washington, DC, 1974, Chap. 25.

[5]Tesner, P. A., Snegiriova, T. D., and Knorre, V. G., "Kinetics of Dispersed Carbon Formation," *Combustion and Flame*, Vol. 17, No. 2, 1971, pp. 253–260.

[6]Magnussen, B. F., and Hjertager, B. H., "On Mathematical Modelling of Turbulent Combustion with Special Emphasis on Soot Formation and Combustion," *16th Symposium (International) on Combustion*, The Combustion Inst., Pittsburgh, PA, 1977, pp. 719–728.

[7]Ahmad, T., Plee, S. L., and Myers, J. P., "Computation of Nitric Oxide and Soot Emissions from Turbulent Diffusion Flames," *Journal of Engineering for Gas Turbines and Power*, Vol. 107, No. 1, 1985, pp. 48–53.

[8]Gore, J. P., and Faeth, G. M., "Structure and Spectral Radiation Properties of Turbulent Ethylene/Air Diffusion Flames," *21st Symposium (International) on Combustion*, The Combustion Inst., Pittsburgh, PA, 1986, pp. 1521–1531.

[9]Kent, J. H., and Honnery, D., "Soot and Mixture Fraction in Turbulent Diffusion Flames," *Combustion Science and Technology*, Vol. 54, Nos. 1–6, 1987, pp. 383–397.

[10]Kennedy, I., Kollmann, W., and Chen, J.-Y., "A Model for Soot Formation in a Laminar Diffusion Flame," *Combustion and Flame*, Vol. 81, No. 1, 1990, pp. 73–85.

[11]Kennedy, I., Kollmann, W., and Chen, J.-Y., "Predictions of Soot in Laminar Diffusion Flames," *AIAA Journal*, Vol. 29, No. 9, 1991, pp. 1452–1457.

[12]Villasenor, R., and Kennedy, I. M., "Soot Formation and Oxidation in Laminar Diffusion Flames," *24th Symposium (International) on Combustion*, The Combustion Inst., Pittsburgh, PA, 1992, pp. 1023–1030.

[13]Axelbaum, R. L., Flower, W. L., and Law, C. K., "Dilution and Temperature Effects of Inert Addition on Soot Formation in a Counterflow Diffusion Flame," *Combustion Science and Technology*, Vol. 61, No. 1, 1988, pp. 51–74.

[14]Honnery, D. R., and Kent, J. H., "Soot Mass Growth Modeling in Laminar Diffusion Flames," *24th Symposium (International) on Combustion*, The Combustion Inst., Pittsburgh, PA, 1992, pp. 1041–1047.

[15]Honnery, D. R., Tappe, M., and Kent, J. H., "Two Parametric Models of Soot Growth Rates in Laminar Ethylene Diffusion Flames," *Combustion Science and Technology*, Vol. 83, Nos. 4–6, 1992, pp. 305–321.

[16]Moss, J. B., Stewart, C. D., and Syed, K. J., "Flamelet Chemistry Modeling of Soot Formation for Radiation Prediction in Combustor Flow Fields," CP-422, AGARD, 1987 (Paper 18).

[17]Moss, J. B., Stewart, C. D., and Syed, K. J., "Flowfield Modeling of Soot Formation at Elevated Pressure," *22nd Symposium (International) on Combustion*, The Combustion Inst., Pittsburgh, PA, 1988, pp. 413–423.

[18]Syed, K. J., Stewart, C. D., and Moss, J. B., "Modeling Soot Formation and Thermal Radiation in Buoyant Turbulent Flames," *23rd Symposium (International) on Combustion*, The Combustion Inst., Pittsburgh, PA, 1990, pp. 1533–1541.

[19]Stewart, C. D., Syed, K. J., and Moss, J. B., "Modeling Soot Formation in Non-Premixed Kerosene-Air Flames," *Combustion Science and Technology*, Vol. 75, Nos. 4–6, 1991, pp. 211–226.

[20]Leung, K. M., Lindstedt, R. P., and Jones, W. P., "A Simplified Reaction Mechanism for Soot Formation in Non-Premixed Flames," *Combustion and Flame*, Vol. 87, Nos. 3, 4, 1991, pp. 289–305.

[21]Fairweather, M., Jones, W. P., and Lindstedt, R. P., "Predictions of Radiative Transfer from a Turbulent Reacting Jet in a Cross-Wind," *Combustion and Flame*, Vol. 89, No. 1, 1992, pp. 45–63.

[22]Fairweather, M., Jones, W. P., Ledin, H. S., and Lindstedt, R. P., "Predictions of Soot Formation in Turbulent, Non-Premixed Propane Flames," *24th Symposium (International) on Combustion*, The Combustion Inst., 1992, pp. 1067–1074.

[23]Missaghi, M., Pourkashanian, M., Smedley, J. M., Williams, A., and Yap, L. T., "A Computational Study of Soot Formation in Turbulent Diffusion Flames," *Proceedings of the 2nd International Conference on Combustion Technologies for a Clean Environment*, Lisbon, Portugal, 1993 (Paper 34.2).

[24]Nishida, O., and Mukohara, S., "Characteristics of Soot Formation and Decomposition in Turbulent Diffusion Flames," *Combustion and Flame*, Vol. 47, No. 3, 1982, pp. 269–279.

[25]Nagle, J., and Strickland-Constable, R. F., "Oxidation of Carbon Between 1000°–2000°C," *Proceedings of the 5th Conference on Carbon*, Vol. 1, Pergamon, London, 1962, pp. 154–164.

[26]Lee, K. B., Thring, M. W., and Beer, J. M., "On the Rate of Combustion of Soot in a Laminar Soot Flame," *Combustion and Flame*, Vol. 6, 1962, pp. 137–145.

[27]Neoh, K. G., Howard, J. B., and Sarofim, A. F., "Soot Oxidation in Flames," *Particulate Carbon Formation During Combustion*, edited by D. C. Siegla and G. W. Smith, Plenum, New York, 1981.

[28]Garo, A., Prado, G., and Lahaye, J., "Chemical Aspects of Soot Particles Oxidation in a Laminar Methane-Air Diffusion Flame," *Combustion and Flame*, Vol. 79, Nos. 3, 4, 1990, pp. 226–233.

[29]Bradley, D., Dixon-Lewis, G., Habik, S., and Mushi E., "The Oxidation of Graphite Powder in Flame Reaction Zones," *20th Symposium (International) on Combustion*, The Combustion Inst., Pittsburgh, PA, 1984, pp. 931–940.

[30]Pope, S. B., "An Explanation of the Turbulent Round-Jet/Plane-Jet Anomaly," *AIAA Journal*, Vol. 16, No. 3, 1978, pp. 279–291.

[31]Kaplan, C. R., Baek, S. W., Oran, E. S., and Ellzey, J. L., "Dynamics of a Strongly Radiating Unsteady Ethylene Jet Diffusion Flame," *Combustion and Flame*, Vol. 96, Nos. 1, 2, 1994, pp. 1–21.

[32]Sivathanu, Y. R., and Gore, J. P., "Coupled Radiation and Soot Kinetics Calculations in Laminar Acetylene/Air Diffusion Flames," *Combustion and Flame*, Vol. 97, 1994, pp. 161–172.

[33]Gore, J. P., Ip, U.-S., and Sivathanu, Y. R., "Coupled Structure and Radiation Analysis of Acetylene/Air Flames," *Journal of Heat Transfer*, Vol. 114, No. 2, 1992, pp. 487–493.

[34]Crauford, N. L., Liew, S. K., and Moss, J. B., "Experimental and Numerical Simulation of a Buoyant Fire," *Combustion and Flame*, Vol. 61, No. 1, 1985, pp. 63–77.

[35]Abbas, A. S., "The Prediction of the Performance of Heavy Oil-Fired Combustors," Ph.D. Dissertation, Univ. of London, London, 1982.

[36]Dalzell, W. D., Williams, G. C., and Hottel, H. C., "A Light-Scattering Method for Soot Concentration Measurements," *Combustion and Flame*, Vol. 14, 1970, pp. 161–170.

[37]Abbas, A. S., and Lockwood, F. C., "Prediction of Soot Concentration in Turbulent Diffusion Flames," *Journal of the Institute of Energy*, Vol. LVIII, Sept. 1985, pp. 112–115.

[38]Vandsburger, U., Kennedy, I. M., and Glassman, I., "Sooting Counterflow Diffusion Flames with Varying Oxygen Index," *Combustion Science and Technology*, Vol. 39, Nos. 1–6, 1984, pp. 263–285.

[39]Glassman, I., "Soot Formation in Combustion Processes," *22nd Symposium (International) on Combustion*, The Combustion Inst., Pittsburgh, PA, 1988, pp. 295–311.